

# Nanostructuration of ionic liquids in fluorinated matrix: Influence on the mechanical properties

Sébastien Livi<sup>a,b,c,\*</sup>, Jannick Duchet-Rumeau<sup>a,b,c</sup>, Jean-François Gérard<sup>a,b,c</sup>

<sup>a</sup> Université de Lyon, F-69003 Lyon, France

<sup>b</sup> INSA Lyon, F-69621 Villeurbanne, France

<sup>c</sup> CNRS, UMR 5223, Ingénierie des Matériaux Polymères, France

## ARTICLE INFO

### Article history:

Received 7 October 2010

Received in revised form

13 January 2011

Accepted 29 January 2011

Available online 24 February 2011

### Keywords:

Ionic liquid

Building block

Nanostructuration

## ABSTRACT

In this work, a new method to prepare fluorinated coatings with mechanical properties enhanced has been developed. Pyridinium, imidazolium, and phosphonium ionic liquids have been synthesized and used as new synthetic building blocks in a polytetrafluoroethylene matrix. The strategy demonstrated using long alkyl chain cations provides an opportunity to prepare nanomaterials with a nanoscale structuration. The design of these new ionic and nanostructured materials is very dependent on the cation–anion combination of ILs. The morphology analyzed by transmission electronic microscopy (TEM) shows that it is clearly tuned by the chemical nature of ILs. The finest structuration leads to a dramatic compromise between stiffness and deformation of material. The small-angle X-Ray scattering (SAXS) shows the evolution of the ionic networks during the mechanical sollicitation.

© 2011 Elsevier Ltd. All rights reserved.

## 1. Introduction

In the world of nanotechnology, the goal is to create new materials with significantly improved physical properties from designing matter structuration at nanoscale. For many years, several approaches have been described for designing new structures from organic molecules, polymers, or organic–inorganic hybrids. One of the well-known approach consists in the design of nanostructured thermosets obtained by the use of block copolymers with amphiphilic block [1–3]. Another way for the development of nanostructured polymers is the introduction of inorganic nano-objects having nanometre-scale dimensions such as silica [4], layered silicates [5–10], or carbon nanotubes [11–13]. The problem with these different methods mentioned above is that they require several preparation steps before achieving improved materials. In fact, in the field of the polymer nanocomposites, it is often necessary to modify the surface of the inorganic nanoparticles in order to improve the dispersion as well as the final properties of materials. In the case of thermosets, the synthesis of block copolymers can be long and difficult. Moreover, it is necessary to use large amounts of copolymers to improve properties of the material. To overcome these

obstacles, our research has been directed towards organic compounds with intrinsic and unique properties: Ionic Liquids (ILs) especially known for their excellent thermal stability, non-flammability, low saturated vapour pressure, good electrical, and thermal conductivity and commonly used as green solvents in inorganic synthesis [14] and synthesis of nanoparticles [15], homogeneous and heterogeneous catalysis [16], in polymer science as plasticizers [17], or lubricants [18].

They are also commonly used as surfactants in the lamellar silicate nanocomposites. The most frequently used are ammonium salts [19–21]. In recent years, pyridinium, imidazolium, and phosphonium ionic liquids known for their excellent thermal stability are increasingly used [22,23]. And recently, a new approach of ILs has been studied by Wathier and Grinstaff [24] who have suggested that ionic liquids may play an important role in the formation of ionic networks based on coordinating ion pairs. They have demonstrated that Coulomb interactions are governed by pairwise interactions between cation and anion and the extended structure of the ionic liquid may lead to a supramolecular ionic network. Thus, a combination of the mechanical properties linked to ionomers with the homogeneity and the high charge densities typical of ionic liquids could lead to a new range of optimized materials. However, from our knowledge, no paper described the use of ionic liquids within a polymer matrix to design nanostructured phase. In this paper the synthesis of ionic liquids based on various cation: pyridinium, imidazolium and phosphonium but also on the different anions (hexafluorophosphate, iodide and bromide) has been described.

\* Corresponding author. Cornell University, College of Engineering Materials Science & Engineering, 416 Bard Hall, Ithaca, NY 14853-1501, USA. Tel.: +33 607 255 6684; fax: +33 607 255 2365.

E-mail address: [sebastien.livi@gmail.com](mailto:sebastien.livi@gmail.com) (S. Livi).

Then, their influences in a fluorinated matrix, chosen for coating applications as well as the consequences of this structuration at nanoscale on the material physical behaviour such as mechanical properties have been studied.

## 2. Experimental

### 2.1. Materials

All chemicals used for to the synthesis of ionic liquids, i.e. triphenylphosphine (95%), imidazole (99.5%), pyridine (99%), iodoctadecyl (95%) and all the solvents (toluene, sodium methanoate, pentane and acetonitrile) were supplied from Aldrich and used as received. The polytetrafluoroethylene used in this study, denoted as PTFE, is an aqueous dispersion of PTFE from Solvay. The composition is as follows: PTFE (60 wt %), water (32–33 wt %), octylphenol polyethoxylates Triton® (7 wt %) and ammonium perfluorooctanoate (0.1 wt %). The pH of aqueous dispersion is 10 and the PTFE particle average size is about 220 nm.

### 2.2. Synthesis of pyridinium, imidazolium, and phosphonium ionic liquids

The synthesis of 1-octadecyl-3-octadecylimidazolium and octadecyltriphenylphosphonium iodide was obtained from a route similar to that described by Livi et al. [25]. Octadecyltriphenylphosphonium hexafluorophosphate and octadecylpyridinium iodide are not commercially available.

#### 2.2.1. Synthesis of octadecylpyridinium iodide ( $C_{18}PyI^-$ )

These compounds are not commercially available and their synthesis was not reported before. In a 100 mL flask was placed under a nitrogen pressure, 10 mmol of octadecyl iodide ( $C_{18}H_{37}I$ ) and distilled pyridine (1.5 equiv.). The stirred suspension was allowed to react for 24 h at room temperature. A yellow precipitate was formed. The reaction mixture was then filtered, and washed repeatedly with pentane. Most of the solvent was removed under vacuum. A white solid was obtained. After drying, alkyl phosphonium salt was fully characterized by spectroscopy  $^{13}C$  NMR and thermogravimetric analysis (TGA).

$^{13}C$  NMR ( $CDCl_3$ )  $\delta$ : 14.04 ( $CH_3$ ); 22.58; 25.91; 28.99; 29.25–29.60; 31.81–31.84 ( $CH_2$ ); 62.02 ( $CH_2N$ ); 128.57 ( $C$ ); 144.82; 145.50 ( $CN$ ). Yield = 90%, melting temperature ( $^{\circ}C$ ): 102  $^{\circ}C$ . The degradation temperature of the  $C_{18}PyI^-$  determined for a weight loss of 50 wt % is 270  $^{\circ}C$ .

#### 2.2.2. Synthesis of 1-octadecyl-3-octadecylimidazolium iodide ( $C_{18}C_{18}ImI^-$ )

A solution of sodium methoxide was prepared from sodium (1 equiv.) in dry freshly distilled methyl alcohol (10 mL) in a sealed septum, 100 mL round-bottomed, three necked flask equipped with a condenser, under nitrogen atmosphere and magnetic stirring. Imidazole (1 equiv.) diluted in acetonitrile (10 mL) was then added into the stirred mixture of sodium methoxide previously cooled at room temperature. After 15 min, a white precipitate was formed. The suspension was then concentrated under reduced pressure for 1 h. The dried white powder was dissolved in acetonitrile and a powder of alkyl iodide (1 equiv.) diluted in acetonitrile (10 mL) was then added under an inert atmosphere of nitrogen at room temperature. The mixture was stirred for 1 h, then heated under reflux at 85  $^{\circ}C$  for about 24 h. A powder of alkyl iodide (1 equiv.) diluted in acetonitrile (10 mL) was added to the mixture at room temperature. The stirred suspension was heated under reflux at 85  $^{\circ}C$  for about 24 h leaving a brownish viscous oil in each case. After cooling to room temperature, the solvent was removed by

evaporation under vacuum, the beige coloured powder was filtered, washed repeatedly with pentane and dried. Purification of the resulting imidazolium salts was accomplished by crystallization from ethyl acetate/acetonitrile: 75/25 mixture. After drying, alkyl imidazolium salt was fully characterized by spectroscopy and thermogravimetric analysis (TGA). The assignment of  $^{13}C$  NMR spectroscopy resonance peaks is an evidence of the success of the ionic liquid synthesis.

2.2.2.1. 1-Octadecyl-3-octadecylimidazolium iodide.  $^{13}C$  NMR ( $CDCl_3$ ):  $\delta$  14.10 ( $2CH_3$ ); 22.67 ( $2CH_2Me$ ); 26.23; 28.97; 29.35–29.69; 30.24; 31.91 ( $CH_2$ ); 50.10; ( $CH_2N$ ); 50.32 ( $CH_2N^-$ ); 121.69; 122.48 ( $CN$ ); 136.88 ( $N-CN$ ). Yield = 94%, melting temperature ( $^{\circ}C$ ): 67  $^{\circ}C$ . The degradation temperature of the  $C_{18}C_{18}ImI^-$  determined for a weight loss of 50 wt % is 310  $^{\circ}C$ .

#### 2.2.3. Synthesis of octadecyltriphenylphosphonium iodide, bromide ( $C_{18}P I^-$ , $C_{18}P Br^-$ )

In a 100 mL flask were placed under a positive nitrogen pressure, triphenylphosphine and octadecyl iodide or octadecyl bromide. The stirred suspensions were allowed to react for 24 h at 120  $^{\circ}C$  in toluene (20 mL), a yellow precipitate was formed. The reaction mixture was then filtered, washed repeatedly with pentane. Most of the solvent was removed under vacuum and the product was dried to a constant weight to give a white solid. These salts were characterized by  $^{13}C$  NMR spectroscopy and thermogravimetric analysis (TGA).

2.2.3.1. Octadecyltriphenylphosphonium iodide.  $^{13}C$  NMR ( $CDCl_3$ ):  $\delta$  14.00 ( $CH_3$ ); 22.67 ( $CH_2Me$ ); 23.2; 29.37–29.66; 30.24; 31.85 ( $PCH_2$ ); 118.45; 130.43; 133.70; 135.15 ( $P-Carom.$ ). Yield = 97%, melting temperature ( $^{\circ}C$ ): 86  $^{\circ}C$ .

2.2.3.2. Octadecyltriphenylphosphonium bromide.  $^{13}C$  NMR ( $CDCl_3$ ):  $\delta$  14.00 ( $CH_3$ ); 22.52 ( $CH_2Me$ ); 23.0; 28.90–29.66; 30.20; 32.00 ( $PCH_2$ ); 118.85; 130.80; 133.50; 135.45 ( $P-Carom.$ ). Yield = 88%, melting temperature ( $^{\circ}C$ ): 86  $^{\circ}C$ . The degradation temperature of the  $C_{18}P I^-$  and  $C_{18}P Br^-$  determined for a weight loss of 50 wt % is 320  $^{\circ}C$ .

#### 2.2.4. Synthesis of octadecyltriphenylphosphonium hexafluorophosphate ( $C_{18}P PF_6^-$ )

In a 100 mL flask, octadecyl iodide ( $C_{18}H_{37}I$ ) (5.0 g, 1 equiv.) was dissolved into dichloromethane (25 mL). The mixture was stirred for 30 min at room temperature. A solution of hydrogen hexafluorophosphate ( $HPF_6$ ) (3.8 g, 2 equiv.) diluted in water (25 mL) was stirred for 30 min and added to the octadecyl iodide solution. The stirred suspension was allowed to react for 24 h at room temperature. The reaction mixture was then introduced in a separatory funnel and the organic layer was washed repeatedly with distilled water ( $4 \times 25$  mL). The mixture was dried over anhydrous magnesium sulphate and concentrated under reduced pressure. The solvent was removed by evaporation under vacuum and the product was dried to a constant weight to give a white solid. The salt was characterized by  $^{13}C$  NMR spectroscopy and thermogravimetric analysis (TGA).

2.2.4.1. Octadecyltriphenylphosphonium hexafluorophosphate.  $^{13}C$  NMR ( $CDCl_3$ ):  $\delta$  14.00 ( $CH_3$ ); 22.35 ( $CH_2Me$ ); 23.5; 29.12–29.74; 30.35; 31.75 ( $PCH_2$ ); 118.75; 130.22; 133.50; 135.05 ( $P-Carom.$ ). Yield = 80%, melting temperature ( $^{\circ}C$ ): 80  $^{\circ}C$ . The degradation temperature of the  $C_{18}P PF_6^-$  determined for a weight loss of 50 wt % is 450  $^{\circ}C$ .

In this work, different combinations cation/anion are proposed and are summarized in Fig. 1.

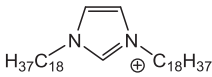
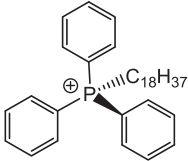
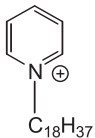
Cation	Anion	Designation
	$\Gamma^-$	$C_{18}C_{18}Im \Gamma^-$
	$\Gamma^-$ $Br^-$ $PF_6^-$	$C_{18}P \Gamma^-$ $C_{18}P Br^-$ $C_{18}P PF_6^-$
	$\Gamma^-$	$C_{18}Py \Gamma^-$

Fig. 1. Structure of the ionic liquids.

### 2.3. Processing and characterization of the IL/PTFE films

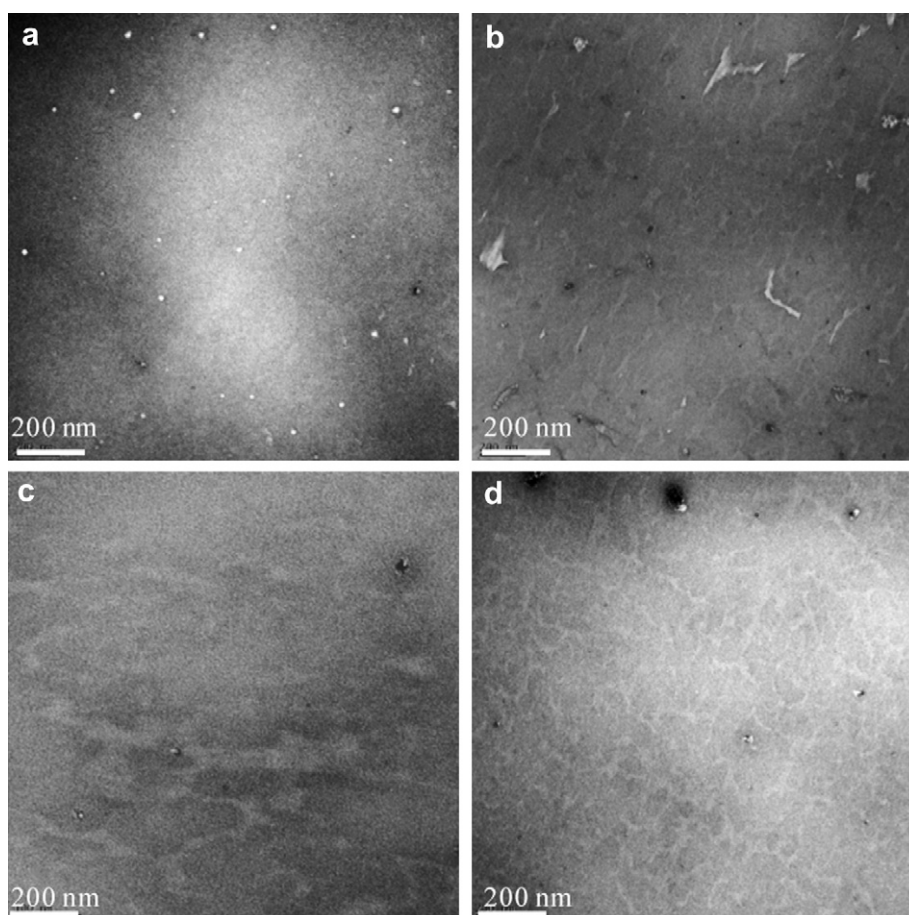
The aqueous suspensions of PTFE containing 1 wt% of pyridinium or imidazolium or phosphonium ionic liquids were agitated by a Rayneri® disperser with a speed of 1500 rpm for 15 min. Then the suspension was spread on stainless steel plates with a bar coater equipped with a bar of 50 microns in order to get 20 microns-thick dried films. A thermal treatment at 400 °C for 10 min was necessary to obtain the polymer film.

**Thermogravimetric analysis (TGA)** performed on the ionic liquids and on PTFE/IL nanocomposites were performed by using Q500 thermogravimetric analyser (TA instruments). The samples were heated to 700 °C at a rate of 20 K min<sup>-1</sup> under nitrogen flow of 90 mL/min.

**DSC measurements** were carried out by using Q20 (TA instruments) in the range of -20 °C to 400 °C. The samples were kept for 3 min at 400 °C to erase the thermal history before being heated or cooled at a rate of 10 K min<sup>-1</sup> under nitrogen flow of 50 mL/min. For calculations of enthalpy of melting and crystallization, the enthalpy of reference used for PTFE is 82 J/g [19,20].

**Wide angle X-ray diffraction spectra (WAXD)** were carried out on a Bruker D8 Advance X-ray diffractometer at the H. Longchambon diffractometry centre at room temperature. A bent quartz monochromator was used to select the Cu K<sub>α1</sub> radiation (=0.15406 nm) and run under operating conditions of 45 mA and 33 kV in Bragg–Brentano geometry. The angle range analyzed was from 1 to 30° 2θ.

**Small-Angle X-ray Scattering** was carried out on the D2AM beam-line at the European synchrotron Radiation Facility (ESRF, Grenoble, France). The incident photon energy was 16 keV. A bidimensional

Fig. 2. TEM micrographs of neat PTFE (a) and blends PTFE/ $C_{18}C_{18}Im \Gamma^-$  (b), PTFE/ $C_{18}Py \Gamma^-$  (c), PTFE/ $C_{18}P \Gamma^-$  (d).

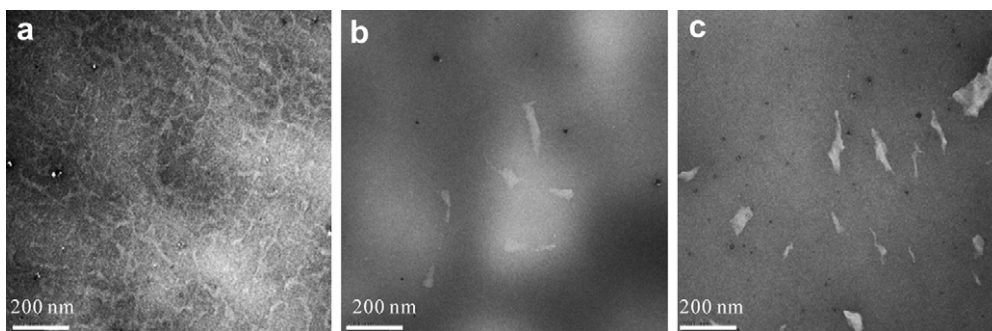


Fig. 3. TEM micrographs of blends PTFE/C<sub>18</sub>P I<sup>−</sup> (a), PTFE/C<sub>18</sub>P Br<sup>−</sup> (b), PTFE/C<sub>18</sub>P PF<sub>6</sub><sup>−</sup> (c).

detector (CCD camera from Ropper Scientific) was used to collect the scattered radiation. The contribution of the empty cell was subtracted from the scattering images of the studied samples.

X-ray Photoelectron Spectroscopy experiments were carried out in a KRATOS AXIS Ultra DLD spectrometer using a hemispherical analyzer and working at a vacuum better than  $10^{-9}$  mbar. All the data were acquired using monochromated Al K $\alpha$  X-rays (1486.6 eV, 150 W), a pass energy of 40 eV, and a hybrid lens mode. The area analysed is  $700 \mu\text{m} \times 300 \mu\text{m}$ . The peaks were referenced to the C–(C,F) components of the C1s band at 284.6 eV.

The Transmission Electron microscopy (TEM) was collected at the Centre of Microstructures (Université de Lyon) on a Philips CM 120 field emission scanning electron microscope with an accelerating voltage of 80 kV. The samples were cut using an ultramicrotome equipped with a diamond knife, to obtain 60 nm thick ultrathin sections. Then, the sections were set on copper grids for observation.

Tensile property tests were carried out on an MTS 2/M electro-mechanical testing system at  $22 \pm 1$  °C and  $50 \pm 5\%$  relative humidity at crosshead speed of  $0.004$  and  $0.2 \text{ s}^{-1}$ . A cookie cutter was used to obtain dumbbell-shaped specimens.

Dynamic Mechanical Thermal Analysis was carried out on a Rheometrics Solid Analyzer RSA II at 0.01% tensile strain and a frequency of 1 Hz. The heating rate was 3 K/min for the temperature range from  $-130$  °C to  $320$  °C.

### 3. Results and discussion

#### 3.1. Effect of ionic liquids on the structuration of fluorinated polymer films

##### 3.1.1. Bulk nanostructures evidenced by transmission electronic microscopy (TEM)

Transmission electron microscopy is the suitable tool to reveal the existence of ILs as a separated phase into the fluorinated matrix according to the difference in electronic densities. With only 1 wt % of ILs, a structuration is reached (Fig. 2). In this study, the chemical nature of the cation and halide anions plays a key role on the different morphologies obtained. The dispersion of imidazolium ionic liquid (C<sub>18</sub>C<sub>18</sub>Im I<sup>−</sup>) generates two types of nanostructuration:

Table 1  
Atomic percentage of species detected on the surface of PTFE films.

Atomic %	C–F	C–C
PTFE	59	30
PTFE 1%	97	3
C <sub>18</sub> P I <sup>−</sup>		
PTFE 5%	93	5
C <sub>18</sub> P I <sup>−</sup>		
PTFE 1%	88	12
C <sub>18</sub> C <sub>18</sub> Im I <sup>−</sup>		

the first one corresponds to the formation of aggregates of ionic clusters while the second one is similar to a co-continuous morphology. A less achieved co-continuous morphology is also obtained with pyridinium ionic liquids (C<sub>18</sub>Py I<sup>−</sup>). In the case of phosphonium ionic liquid, an excellent dispersion is achieved since a structuration at nanoscale is obtained in the polymer matrix.

The use of the different counteranions halide (I<sup>−</sup>, Br<sup>−</sup>) or fluorinated (PF<sub>6</sub><sup>−</sup>) associated to phosphonium cation significantly influences the final morphology as reported in Fig. 3. A poor distribution of important aggregates can be observed with bromide anion whereas a coarse morphology resulting from a good distribution of aggregates is also obtained with the fluorinated anion. Both of these microscale structurations display a large contrast in comparison to the nanoscale morphology reached with the iodide anion.

Due to the hydrophobic nature of polytetrafluoroethylene and strong interactions between ionic compounds in PTFE/IL blends, a phase-separated morphology is generated spontaneously. In fact, in the present case, whatever the ionic liquid considered, their miscibility remains very poor even with the presence of the octadecyl chain. Nevertheless, such morphologies could be compared to the ones observed in ionomers for which ion-containing polymers provide a mean of generation of various types of morphologies and subsequent properties especially in polymer blends [26,27]. In such materials, the ionic species introduce specific interactions between components and could lead to miscible or partially miscible blends of two immiscible polymers from the control of the type of ionic acid group and/or counteranion. It is well known that the clustering of ion pair in a low dielectric constant medium is responsible for different nano- and microstructures which can be predicted theoretically [28,29]. The main parameter controlling the microphase separation in a non-polar media is the dipole–dipole interactions between pairs leading to formation of multiplet structures [30,31], i.e. ionic aggregates. In this study, the same phenomena could be evoked with the formation of ionic liquid aggregates which from different types of morphologies depending on the balance of the interactions between polymer medium and anion–cation pairs.

In conclusion, the ionic liquids have a similar behaviour to ionomers which are well described in the literature [29,30]. As reported, ionic liquids form ionic clusters of varied morphologies from nanoscale up to microscale, easily tuned by the wide variety of salts achieved by a great number of combinations possible between cation and anion.

Table 2  
Influence of organic cation on the physical properties of PTFE films (Std, cooling rate  $10 \text{ K min}^{-1}$ ).

Samples	$T_m$ (°C)	$T_c$ (°C)	$\Delta H_m$ (J/g)	Xc (%)
PTFE	326	310	32	39
PTFE/C <sub>18</sub> P I <sup>−</sup>	328	307	28	34
PTFE/C <sub>18</sub> C <sub>18</sub> Im I <sup>−</sup>	328	307	29	35
PTFE/C <sub>18</sub> Py I <sup>−</sup>	329	308	36	44



**Table 3**

Influence of anion on the physical properties of PTFE films (Std, cooling rate 10 K min<sup>-1</sup>).

Samples	$T_m$ (°C)	$T_c$ (°C)	$\Delta H_m$ (J/g)	Xc (%)
PTFE	326	310	32	39
PTFE/C <sub>18</sub> P I <sup>-</sup>	328	307	28	34
PTFE/C <sub>18</sub> P Br <sup>-</sup>	327	307	28	34
PTFE/C <sub>18</sub> P PF <sub>6</sub> <sup>-</sup>	329	308	31	38

**Table 4**

Dynamical mechanical analysis of IL-modified PTFE: Change of storage moduli at various temperatures at 1 Hz.

Sample	E' (*10 <sup>6</sup> MPa) 25 °C	E' (*10 <sup>6</sup> MPa) 150 °C	E' (*10 <sup>6</sup> MPa) 250 °C
PTFE	505	84	42
PTFE/C <sub>18</sub> P I <sup>-</sup>	405	139	82
PTFE/C <sub>18</sub> P Br <sup>-</sup>	425	138	66
PTFE/C <sub>18</sub> P PF <sub>6</sub> <sup>-</sup>	547	193	99
PTFE/C <sub>18</sub> Im I <sup>-</sup>	594	136	68
PTFE/C <sub>18</sub> Py I <sup>-</sup>	522	141	57

### 3.1.2. Surface analysis by X-ray Photoelectron Spectroscopy (XPS)

According to the chemical nature of the two components, *i.e.* PTFE and ILs, a surface segregation could occur. In order to evaluate the interactions between ILs and fluorinated matrix and a possible enrichment of one of the components at the surface of the films, X-ray photoelectron spectrometry was used to analyze the surface of the neat PTFE and ILs/PTFE films. The Table 1 shows the percentage of C–F and C–C bonds detected on the sample surface.

The neat PTFE composed only of (–CF<sub>2</sub>–CF<sub>2</sub>–) monomer units displays a ratio of two between the C–F (60%) and C–C (30%) bonds. As the ionic liquid is added to the polymer matrix, a significant decrease of C–C bonds in the presence of ionic liquids C<sub>18</sub>C<sub>18</sub>Im I<sup>-</sup>, C<sub>18</sub>P I<sup>-</sup> is observed. With C<sub>18</sub>P I<sup>-</sup>, only 3% of C–C bonds were measured instead of 30% on neat PTFE film which cannot be explained by a surface segregation. These results are an evidence of the influence of ionic liquids on the chain scission due to the formation of HF, HI, HBr acids [32,33], favoured by the fluorinated aqueous suspension. Thus, an increase of C–F bonds during the post-treatment at high temperature is observed. Moreover, the migration of IL takes place in the bulk of the material since no trace of iodine, phosphorous, or nitrogen has been found at the surface even at higher ILs contents, *i.e.* 5 wt %.

## 3.2. Effect of ionic liquids on the PTFE crystallinity

### 3.2.1. Influence of the organic cation

The effect of IL on the polymer physical characteristics such as crystallinity was studied (the samples were analyzed at a heating and a cooling rate of 10 K min<sup>-1</sup>). Table 2 gathers melting ( $T_m$ ) and crystallisation ( $T_c$ ) temperatures as well as the corresponding

enthalpies of melting  $\Delta H_m$ , and crystallization,  $\Delta H_c$ , for the neat fluorinated matrix and with the addition of 1 wt % of the different types of IL.

The IL incorporation into polymer matrix has a minor effect on the thermal transitions. The melting temperatures of neat PTFE or PTFE modified with pyridinium, imidazolium, or phosphonium ionic liquids are included between 326 °C (PTFE) and 329 °C (PTFE/C<sub>18</sub>Py I<sup>-</sup>). Regarding the crystallization temperatures, no significant difference is observed since the values are nearly in the same temperature range, *i.e.* from 307 °C to 310 °C. Only, the chemical nature of organic cation induces differences in the crystallinity of the PTFE matrix. Indeed, the addition of phosphonium and imidazolium ionic liquids results in a slight decrease in crystallinity. This decrease could be attributed to the steric hindrance of cations caused by the presence of two long alkyl chains on imidazolium ion and the presence of three benzyl groups and a long alkyl chain on phosphonium ion. On the other side, octadecylpyridinium iodide that is less hindered has a light nucleating effect on the crystallization of fluoropolymer with an increase of 5%.

### 3.2.2. Influence of halide or fluorinated anions associated to phosphonium cation

The effect of halide (Br<sup>-</sup>, I<sup>-</sup>) or fluorinated (PF<sub>6</sub><sup>-</sup>) anions combined to phosphonium cation on the crystallinity of polymer films was studied by DSC (Table 3).

The melting and crystallization temperatures are not affected by the nature of the anion since the DSC measurements are the same whatever the anion used. In terms of the melting enthalpies, the

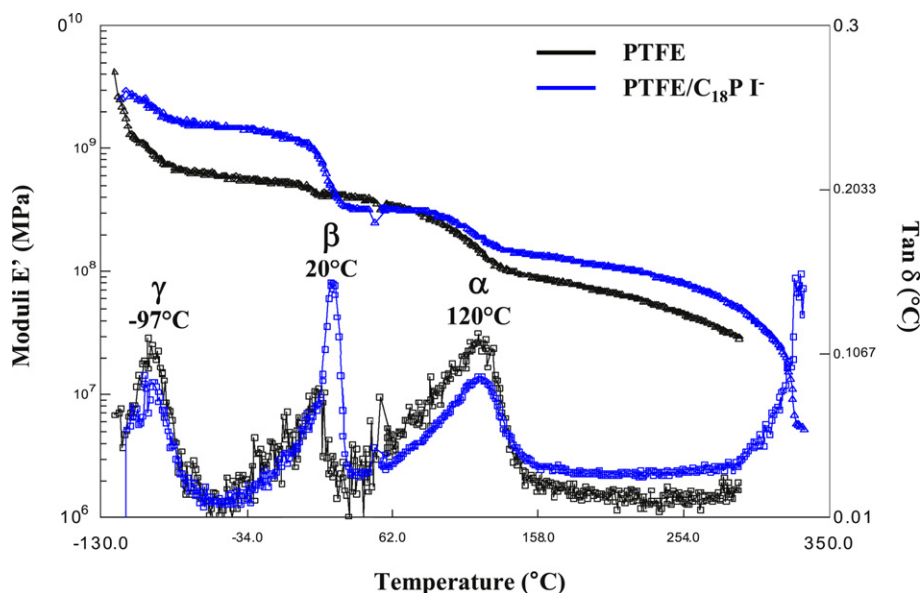


Fig. 4. Storage moduli  $E'$ , main and secondary relaxations of PTFE, PTFE C<sub>18</sub>P I<sup>-</sup> evidenced on  $\tan \delta$  spectra recorded at 1 Hz.

**Table 5**

Effect of ionic liquids on tensile properties of polymer films (1 wt %) (crosshead speed:  $0.004 \text{ s}^{-1}$ ).

Sample	Tensile modulus (MPa) ( $\pm 5$ – $10 \text{ MPa}$ )	Strain at break (%) ( $\pm 10\%$ )
PTFE	65	180
PTFE/C <sub>18</sub> P I <sup>−</sup>	170	522
PTFE/C <sub>18</sub> P Br <sup>−</sup>	120	140
PTFE/C <sub>18</sub> P PF <sub>6</sub> <sup>−</sup>	140	70
PTFE/C <sub>18</sub> C <sub>18</sub> Im I <sup>−</sup>	110	160
PTFE/C <sub>18</sub> Py I <sup>−</sup>	90	160

anion has a predominant effect on the halide or fluorinated anions. This phenomenon could be explained by the fact that the fluorinated nature of the anion improves the compatibility with the matrix and contributes to the matrix crystallization.

### 3.3. Effect of ionic liquids on the mechanical properties of fluorinated polymer

#### 3.3.1. Dynamical mechanical analysis of fluorinated polymer-IL blends

As reported in Fig. 4, the dynamic mechanical spectrum of PTFE and PTFE/C<sub>18</sub>P I<sup>−</sup> display the storage moduli  $E'$  and the main relaxation peaks. These peaks were previously assigned by McCrum to the long range motions *i.e.*  $\alpha$  relaxation at  $120^\circ\text{C}$ , to the  $\beta$  relaxation attributed to the combination of a transition in crystal form and at  $-97^\circ\text{C}$ , the random chain motions is attributed to the  $\gamma$  relaxation [34].

The thermomechanical properties can be significantly improved thanks to the high thermal stability of ionic liquids. The storage moduli,  $E'$ , obtained by DMA at different temperatures are summarized in Table 4.

**3.3.1.1. Influence of cations on dynamical mechanical analysis.** The chemical nature of the organic cation plays a key role on the thermomechanical properties of polytetrafluoroethylene. At  $25^\circ\text{C}$ , the film with the imidazolium ion shows at room temperature the highest in the elastic moduli  $E'$  with an increase of 17% compared to unfilled film and 47% compared to the film filled with phosphonium ion. Then at  $150^\circ\text{C}$ , whatever the organic cation used, similar moduli but always higher than PTFE are obtained. At higher temperatures like  $250^\circ\text{C}$ , the highest values in moduli are measured on the PTFE films filled with the phosphonium ionic liquid because of its better thermal stability than the imidazolium salt one.

**3.3.1.2. Influence of anions on dynamical mechanical analysis.** At room temperature, the addition of phosphonium ionic liquids, whatever the nature of the anion used, causes a decrease in modulus of about

**Table 6**

Influence of the nature of the ionic liquid coupled to the strain rate ( $0.004 \text{ s}^{-1}$ ) on the percentage of crystallinity (Std, cooling rate  $10 \text{ K min}^{-1}$ ).

Samples	$T_m$ ( $^\circ\text{C}$ )	$T_c$ ( $^\circ\text{C}$ )	$\Delta H_m$ (J/g)	Xc (%)
PTFE	326	310	32	39
PTFE $0.004 \text{ s}^{-1}$	327	309	32	39
PTFE/C <sub>18</sub> Py I <sup>−</sup>	329	308	36	44
PTFE/C <sub>18</sub> Py I <sup>−</sup> $0.004 \text{ s}^{-1}$	328	308	38	46
PTFE/C <sub>18</sub> C <sub>18</sub> Im I <sup>−</sup>	328	307	29	35
PTFE/C <sub>18</sub> C <sub>18</sub> Im I <sup>−</sup> $0.004 \text{ s}^{-1}$	328	308	36	44
PTFE/C <sub>18</sub> P I <sup>−</sup>	328	307	28	34
PTFE/C <sub>18</sub> P I <sup>−</sup> $0.004 \text{ s}^{-1}$	328	307	42	51

**Table 7**

Influence of the chemical nature of the anion coupled to the strain rate ( $0.004 \text{ s}^{-1}$ ) on the percentage of crystallinity (Std, cooling rate  $10 \text{ K min}^{-1}$ ).

Samples	$T_m$ ( $^\circ\text{C}$ )	$T_c$ ( $^\circ\text{C}$ )	$\Delta H_m$ (J/g)	Xc (%)
PTFE	326	310	32	39
PTFE $0.004 \text{ s}^{-1}$	327	309	32	39
PTFE/C <sub>18</sub> P Br <sup>−</sup>	327	307	28	34
PTFE/C <sub>18</sub> P Br <sup>−</sup> $0.004 \text{ s}^{-1}$	327	307	34	41
PTFE/C <sub>18</sub> P PF <sub>6</sub> <sup>−</sup>	329	308	31	38
PTFE/C <sub>18</sub> P PF <sub>6</sub> <sup>−</sup> $0.004 \text{ s}^{-1}$	329	308	39	48
PTFE/C <sub>18</sub> P I <sup>−</sup>	328	307	28	34
PTFE/C <sub>18</sub> P I <sup>−</sup> $0.004 \text{ s}^{-1}$	328	307	42	51

20% except for PTFE/C<sub>18</sub>P PF<sub>6</sub><sup>−</sup> that remains in the same order of magnitude as the neat matrix. On the other side, as the temperature increases, the moduli values for the PTFE/IL materials decrease slightly but remain always higher than ones measured on neat PTFE. This improvement is more significant when the fluorinated anion is used. In fact, the hexafluorophosphate anion contributes to higher thermomechanical behaviour of IL-modified PTFE. This phenomenon is even more pronounced at higher temperature.

These changes of storage moduli can be explained by the fact that ionic liquids form in the PTFE medium a separated phase which displays a strong cohesion due to the ionic dipole–dipole interactions. According to the temperature dependence of ionic interactions, the multiplet aggregates which exist at low temperature could exist in a larger range of temperature, *i.e.* to higher temperatures, before reaching the temperature at which ionic forces become too weak to contribute to the stiffness of the material. This hypothesis could be similar to the temperature dependence of storage modulus of ionomers with temperature [26].

#### 3.3.2. Mechanical properties of fluorinated films

The mechanical properties determined on the fluorinated films with 1 wt % of ionic liquids are gathered in Table 5.

**3.3.2.1. Influence of cations on static mechanical analysis.** The mechanical performance is very dependent on the nature of ionic liquids used. In fact, for 1 wt% of pyridinium and imidazolium ions, the mechanical behaviours analysed in uniaxial tension mode are similar. An increase of the modulus of 38% and 41% respectively is obtained with a slight decrease of 11% for the elongation at break. In the opposite, with the phosphonium ionic liquid, surprising results are observed since an increase of 160% of the stiffness and 190% for the strain at break are achieved. The differences of strain at break have been attributed to the distributions of the ionic liquid phase in a polymer film. Thus, the co-continuous morphologies of pyridinium and imidazolium salts lead to a decrease of the elongation at break while the ‘spider web’ morphology obtained with the phosphonium ionic liquid amplifies the plasticization of the polymer matrix. To explain the increases in Young’s modulus of the different systems,

**Table 8**

DSC data on fluorinated films strained at different strain rate ( $0.004$  and  $0.2 \text{ s}^{-1}$ ) (Std, cooling rate  $10 \text{ K min}^{-1}$ ).

Samples	$T_m$ ( $^\circ\text{C}$ )	$T_c$ ( $^\circ\text{C}$ )	$\Delta H_m$ (J/g)	Xc (%)
PTFE without strain	326	310	32	39
PTFE $0.004 \text{ s}^{-1}$	327	309	32	39
PTFE $0.2 \text{ s}^{-1}$	329	308	40	49
PTFE C <sub>18</sub> P I <sup>−</sup> without strain	328	307	28	34
PTFE C <sub>18</sub> P I <sup>−</sup> $0.004 \text{ s}^{-1}$	328	307	42	51
PTFE C <sub>18</sub> P I <sup>−</sup> $0.2 \text{ s}^{-1}$	329	308	49	60

**Table 9**  
Effect of the strain rate on tensile properties of the polymer films.

Sample	Tensile modulus (MPa)	Strain at break (%)
PTFE 0.004 s <sup>-1</sup>	65	180
PTFE 0.2 s <sup>-1</sup>	170	450
PTFE/C <sub>18</sub> P I <sup>-</sup> 0.004 s <sup>-1</sup>	170	522
PTFE/C <sub>18</sub> P I <sup>-</sup> 0.2 s <sup>-1</sup>	200	715

the evolution of the percentage of crystallinity has been studied under mechanical strain (Table 6).

These results clearly demonstrate that when the films are submitted to a strain rate of 0.004 s<sup>-1</sup>, a significant increase of the crystallinity ratio is obtained whatever the chemical nature of the organic cation used. In conclusion, the presence of ionic phase in the polytetrafluoroethylene matrix generates a phenomenon of crystallization under strain. However, better interactions seem to take place between the phosphonium ionic liquid functionalized with long alkyl chains and the fluorinated matrix.

**3.3.2.2. Influence of anion on static mechanical analysis.** The mechanical properties can be also tailored from the chemical nature of the anion. By using the phosphonium ionic liquid, differences are observed for Young's modulus and the strain at break as a function of the anion used. For the three anions, a strong increase of modulus is obtained of 160% with C<sub>18</sub>P I<sup>-</sup>, 84% with C<sub>18</sub>P Br<sup>-</sup> and 115% with C<sub>18</sub>P PF<sub>6</sub><sup>-</sup>. On the other hand, for the strain at break, the phosphonium ionic liquid containing iodide anion has a plasticizing effect with a large increase (190%) whereas for the C<sub>18</sub>P Br<sup>-</sup> and C<sub>18</sub>P PF<sub>6</sub><sup>-</sup>, the addition of these salts reduces the fracture behaviour of the fluorinated matrix with a decrease of 22% and 84% respectively.

These results are consistent with the morphologies shown previously and the DSC data presented in Table 7. In fact, in the case of phosphonium ionic liquid combined with the iodide anion, a very

fine structuration and the largest increase in the percentage of crystallinity lead to better mechanical results. Whereas for C<sub>18</sub>P Br<sup>-</sup> and C<sub>18</sub>P PF<sub>6</sub><sup>-</sup>, the presence of many well-dispersed ionic aggregates in the matrix explain the higher decrease at the strain at break as observed in ionomers [35].

### 3.3.3. Effect of strain rate on the uniaxial tension behaviour of polymer/IL films

**3.3.3.1. Effect of phosphonium ionic liquid on the mechanical and the crystallinity properties.** Due to the fine dispersion of the phosphonium ionic liquid in the fluorinated film and the excellent mechanical compromise achieved, the effects of strain rate were investigated on the Young's modulus and ultimate properties as well as on the morphology changes after uniaxial stretching at a given strain. In fact, DSC measurements after deformation at different strain rates are listed in Table 8 and the mechanical properties are summarized in Table 9.

First of all, one can remember that the PTFE films are not oriented due to the processing method, *i.e.* drying from a water-based solution followed by heating at 400 °C. At low strain rates, the melting enthalpy of the neat PTFE is unmodified, whereas as the fluoropolymer is strained at high strain rates, crystallization under strain takes place. Indeed, the high strain rate applied promotes chain extension which leads to an increase of crystallinity in the polymer. This increase in crystallinity rate could be associated to an increase of Young's modulus from 65 at 170 MPa.

The addition of phosphonium ionic liquid in the fluoropolymer enhances the crystallization under strain with an increase of 10% compared to the neat polymer film. This increase could be due to a rearrangement of the ionic liquid aggregates in the polymer matrix. In fact, the ionic interactions have a reversible character and the ionic liquid phase based on multiplet aggregates could be reorganized continuously during strain. Regarding mechanical

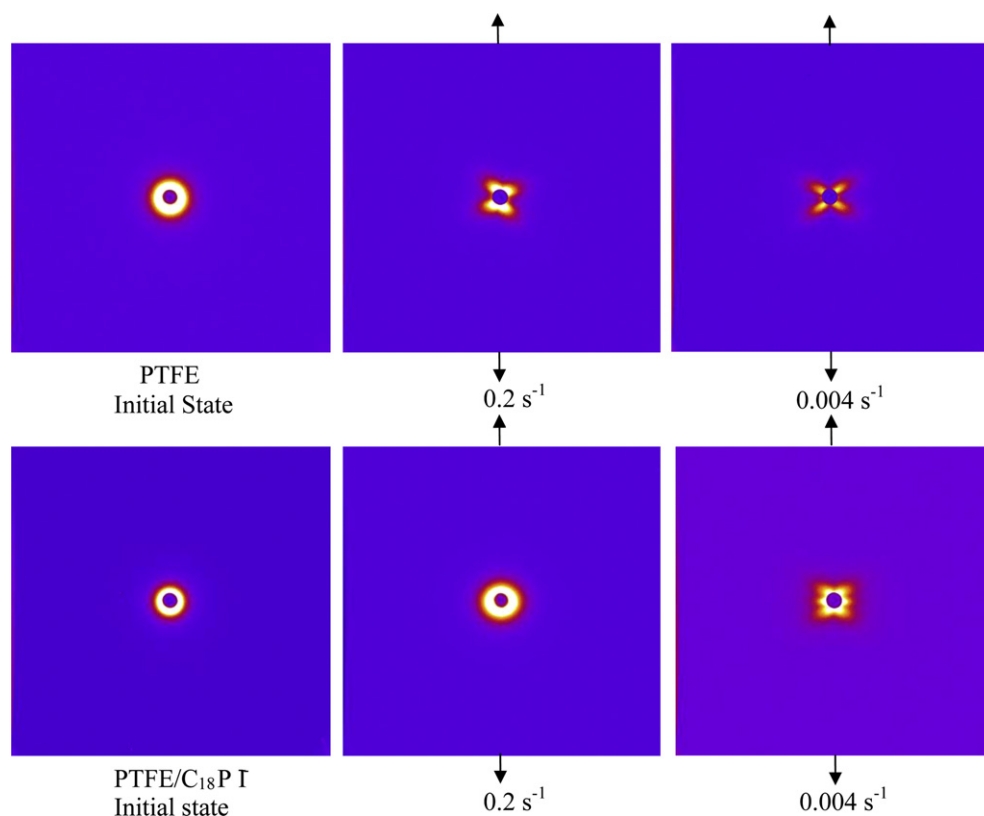


**Fig. 5.** SAXS patterns of neat PTFE and PTFE/C<sub>18</sub>P I<sup>-</sup> under different strain rates. (arrows indicate the axis of uniaxial tension).

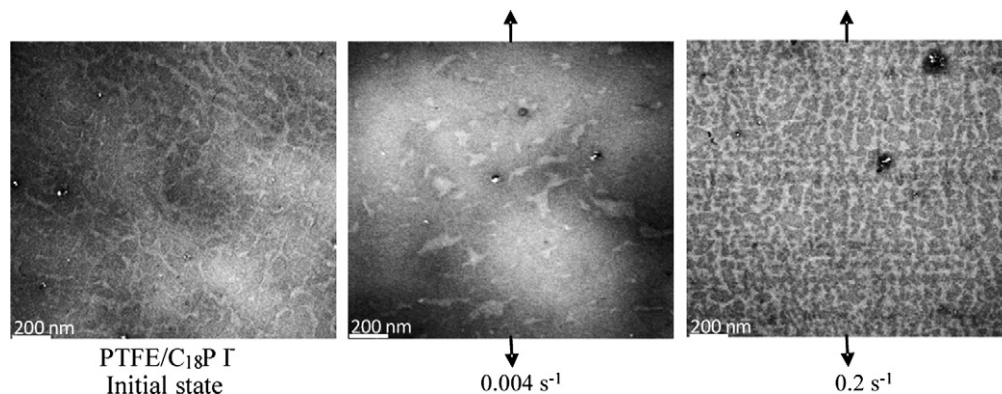


Fig. 6. TEM micrographs of PTFE/C<sub>18</sub>P I<sup>−</sup> under different strain rates (arrows indicate tension axis).

properties, this slight increase in the modulus at high strain rate could reflect the effect of competition between relaxation for the re-organization of ionic liquid phase and deformation.

### 3.3.4. Effect of ionic liquids on the morphology after deformation

For a better understanding of the material change during uniaxial tensile test, SAXS analysis were performed on the PTFE films with and without IL after deformation reached at different deformation rates as reported by Visser and al [36] for ionomers.

The SAXS images performed on unfilled PTFE and PTFE/C<sub>18</sub>P I<sup>−</sup> at different strain rates, *i.e.* 0, 0.004, 0.2 s<sup>−1</sup> are shown in Fig. 5.

Without deformation, the isotropic character of the PTFE film due to the processing method used is observed. As a strain rate (even low) is applied, a configuration with four leaf clover is observed and in presence of ionic liquid, a different organization is noticed. Indeed, without strain, the PTFE/C<sub>18</sub>P I<sup>−</sup> sample shows an anisotropic behaviour that is kept at low strain rates. At a strain rate of 0.2 s<sup>−1</sup>, this phenomenon disappears in favour of an anisotropic behaviour oriented in six directions. As a consequence, the presence of ionic liquid as a dispersed nanophase which is based on multiplet clusters could be used to modify the deformation phenomena of PTFE due to the dynamic character of this phase under strain.

The transmission electron microscopy is used to evidence the morphology of the film. Fig. 6 shows the different morphologies observed on the strained sample after uniaxial test done at different strain rates.

After deformation with a low strain rate, TEM micrographs reveal that the IL nanodomains which are initially organized as a co-continuous nanostructure ('spider web'-type) collapse to form large domains whereas for high strain rate, the IL co-continuous nanostructure is kept and is oriented according to the axis of tension. This means that the relaxation of the IL nanostructures has a relaxation time longer than the characteristic time of the deformation process. This phenomenon could be very close to the ones observed by Visser and Cooper [36] who purposed for ionomers a model invoking ionic aggregate spatial rearrangement within the polymer matrix. The authors also pointed out the role of the nature of ionic pairs on the mechanical deformation behaviour of the fluorinated matrix.

## 4. Conclusions

In this work, new specific building blocks based on pyridinium, imidazolium and phosphonium ionic liquids have been synthesized in order to prepare nanostructured materials. In fact, the use of ionic liquids leads to a structuration at nanoscale into a polymer film

coupled to different mechanical behaviours observed. Thus, we have clearly demonstrated that the effects of the chemical nature of ionic liquid determined by a choice of the cation: pyridinium, imidazolium versus phosphonium and a choice of the anion halide versus fluorinated play a significant role on the structuration and the physical properties of the polymer. Typically, a co-continuous morphology as is the case for the pyridinium and imidazolium salts generates a decrease in strain at break. In opposite, the spider web morphology obtained for the phosphonium ionic liquid with iodide anion lead to a dramatic plasticization (+190%) of the fluorinated matrix. We have also demonstrated that the chain scission caused by the formation of HBr, HI, HF acids during the heat treatment of fluorinated coatings induced crystallization under strain which is responsible of the Young's modulus increase. To conclude this study, we have showed that it is possible to achieve polymer film with an unprecedented flexibility and a stiffness dramatic improvement by using a very small amount of ionic liquid (1 wt %) and that moreover does not really require any special conditions for their synthesis. These new building blocks must open a new alternative in material field for various applications and will be the subject of many studies in the future.

## References

- [1] Guo Q, Liu J, Chen L, Wang K. *Polymer* 2008;49:1737–42.
- [2] Yang X, Yi F, Xin Z, Zheng S. *Polymer* 2009;50:4089–100.
- [3] Xu Z, Zheng S. *Polymer* 2007;48:6134–44.
- [4] Yokoyama R, Suzuki S, Shirai K, Yamauchi T, Tsubokawa N, Tsuchimochi M. *European Polymer Journal* 2006;42:3221–9.
- [5] Priya L, Jog JP. *Journal of Applied Polymer Science* 2003;89:2036–40.
- [6] Pavlidou S, Papaspyrides CD. *Progress in Polymer Science* 2008;33:1119–98.
- [7] Sharma S, Komarneni S. *Applied Clay Science* 2009;42:553–8.
- [8] Stoeffler K, Lafleur PG, Denault J. *Polymer Engineering & Science* 2008;48:1449–66.
- [9] Wang WS, Chen HS, Wu YW, Tsai TY, Chen-Yang YW. *Polymer* 2008;49:4826–36.
- [10] Fu H-K, Huang C-F, Huang J-M, Chang F-C. *Polymer* 2008;49:1305–11.
- [11] Li L, Li B, Hood MA, Li CY. *Polymer* 2009;50:953–65.
- [12] Spitalsky Z, Tasis D, Papagelis K, Galiotis C. *Progress in Polymer Science* 2010;35:357–401.
- [13] Bose S, Khare RA, Moldenaers P. *Polymer* 2010;51:975–93.
- [14] Vallette H, Ferron L, Coquerel G, Gaumont A-C, Plaquevent J-C. *Tetrahedron Letters* 2004;45:1617–9.
- [15] Safavi A, Zeinali S. *Colloids and Surfaces A: Physicochemical and Engineering Aspects* 2010;362:121–6.
- [16] Xu L, Ou G, Yuan Y. *Journal of Organometallic Chemistry* 2008;693:3000–6.
- [17] Rahman M, Brazel CS. *Polymer Degradation and Stability* 2006;91:3371–82.
- [18] Park K, Ha JU, Xanthos M. *Polymer Engineering & Science* 2010;50:1105–10.
- [19] Vazquez A, López M, Kortaberria G, Martín L, Mondragon I. *Applied Clay Science* 2008;41:24–36.
- [20] He H, Duchet J, Galy J, Gerard JF. *Journal of Colloid and Interface Science* 2006;295:202.
- [21] Xie W, Gao Z, Pan WP, Hunter D, Singh A, Vaia R. *Chemistry of Materials* 2001;13(9):2979.
- [22] Awad WH, Gilman JW, Nyden M, Harris RH, Sutto TE, Callahan J, et al. *Thermochimica Acta* 2004;409:3–11.



- [23] Xie W, Xie R, Pan W-P, Hunter D, Koene B, Tan L-S, et al. *Chemistry of Materials* 2002;14:4837–45.
- [24] Wathier M, Grinstaff MW. *Journal of the American Chemical Society* 2008;130:9648.
- [25] Livi S, Duchet-Rumeau J, Pham T-N, Gérard J-F. *Journal of Colloid and Interface Science* 2010;349(1):424–33.
- [26] Bazuin CG, Eisenberg A. *Industrial & Engineering Chemistry Product Research and Development* 1981;16:41.
- [27] Capek I. *Advances in Colloid and Interface Science* 2005;118:73.
- [28] Khokhlov AR, Dormidontova EF. *Physics Uspekhi* 2005;118:73.
- [29] Nyrkova IA, Khokhlov AR, Kramarenko YY. *Polymer Science USSR* 1990;32:852.
- [30] Eisenberg A, Hird B, Moore RB. *Macromolecules* 1990;23:4098.
- [31] Nyrkova IA, Khokhlov AR, Doi M. *Macromolecules* 1993;26:3601.
- [32] Swatloski RP, Holbrey JD, Rogers RD. *Green Chemistry* 2003;5:361–3.
- [33] Lall S, Behaj V, Mancheno D, Casiano R, Thomas M, Rikin A, et al. *Synthesis* 2002;11:1530.
- [34] McCrum NG. *Journal of Polymer Science* 1959;34:355–69.
- [35] Storey RF, Baugh DW. *Polymer* 2000;41(9):3205.
- [36] Visser SA, Cooper SL. *Polymer* 1992;33:4705–10.